

FIG. 1. Results of the experimental runs on the quartz diorite ( $\approx$ andesite) composition in the 0–13.5 kb pressure range.

(3) The albite : anorthite ratio of the feldspar crystallizing is markedly dependent on the pressure of crystallization, with the ratio Ab/An increasing with increasing pressure from 0–13.5 kb for the liquidus and near-liquidus plagioclase (see Fig. 4). No change in Ab/An ratio was detected for the range of temperatures over which the plagioclase crystals were analyzed at any specific pressure.

#### Gabbroic Anorthosite

(1) The results for this composition are summarized in Fig. 2. Analyses are given in Tables IV and V.

(2) The crystallization is dominated by plagioclase up to pressures of 22.5 kb. The corresponding low melting fraction is basic in composition, approximating to an alkali gabbro.

(3) The Ab/An ratio of the liquidus and near-liquidus plagioclase is dependent on the pressure of crystallization, with an increasing Ab/An ratio with increasing pressure, similar to that observed in the quartz diorite composition (Fig. 4). The plagioclase crystallizing from the gabbroic anorthosite composition at a specific pressure shows an increase in Ab/An ratio with decreasing temperature.

(4) There is a large field of crystallization of aluminous clinopyroxene at pressures of 27–36 kb.

#### High-alumina Basalt

(1) The complete results for this composition are summarized in Fig. 3. Analyses of phases crystallizing at 13.5–18 kb are given in Tables VI, VII and VIII. Other results are related to different problems and are discussed elsewhere (Green *et al.* 1967; Green 1967a; Green and Ringwood 1968).

(2) There is a large field of crystallization of aluminous clinopyroxene, especially at 18 kb where pyroxene is the only phase crystallizing for 60 °C below the liquidus.

(3) Clinopyroxene is joined by plagioclase and garnet at 18 kb and plagioclase at 13.5 kb at lower temperatures.

(4) Minor suppression of crystallization of plagioclase occurs in the presence of water.

#### Interpretation of Experimental Results

##### Quartz Diorite

From careful optical examination of the experimental runs, both as powders mounted in

TABLE II

Partial analyses of feldspars from selected runs on the quartz diorite composition (iron content recalculated to zero; soda content calculated)

Conditions of run	13.5 kb	13.5 kb	13.5 kb	13.5 kb	9 kb	9 kb	9 kb	0 kb*	Av. 13.5 kb Composition	Av. 9 kb Composition
	1 hr 1240 °C	1 hr 1220 °C	1 hr 1200 °C	1 hr 1180 °C	1 hr 1200 °C	1 hr 1180 °C	1 hr 1160 °C	1½ hrs 1177 °C		
SiO <sub>2</sub>	57.9	57.3	57.0	58.0	56.4	56.4	56.6	53.6	57.6	56.5
Al <sub>2</sub> O <sub>3</sub>	26.2	26.0	26.4	26.4	27.5	27.5	27.5	29.6	26.3	27.5
CaO	8.1	8.1	8.5	8.2	9.7	9.5	9.5	11.9	8.2	9.6
Na <sub>2</sub> O	6.5	6.4	6.1	6.4	5.6	5.7	5.7	4.6	6.4	5.7
K <sub>2</sub> O	0.7	0.7	0.9	0.8	0.8	0.8	0.8	0.3	0.8	0.8
TOTAL	99.4	98.5	98.9	99.8	100.3	99.9	100.1	100.0	99.3	100.2
Mol. Prop.										
Or	4.1	4.1	5.2	4.6	4.6	4.6	4.6	1.6	4.6	4.6
Ab	56.7	53.6	53.4	55.6	48.6	49.4	49.4	40.7	55.6	49.2
An	39.2	42.3	41.4	39.8	46.8	46.0	46.0	57.7	39.8	46.2

\*Calculated from measured CaO and K<sub>2</sub>O contents.

TABLE III  
Electron microprobe analyses of pyroxenes from selected runs on the quartz diorite composition

Conditions of run	13.5 kb 2 hrs 'Wet' 1180 °C cpx	13.5 kb 2 hrs 'Wet' 1180 °C opx	9 kb 2 hrs 'Wet' 1160 °C opx	9 kb Estimated Composition cpx
SiO <sub>2</sub>	51.1	53.0	53.0*	51.3
TiO <sub>2</sub>	1.2	0.8	0.9	1.2
Al <sub>2</sub> O <sub>3</sub>	8.6	6.1	4.7	5.2
FeO	10.8	11.2	14.8	14.4
MgO	17.2	27.0	23.2	14.9
CaO	10.7	2.6	3.3	12.3
Na <sub>2</sub> O	0.8	—	—	0.7
TOTAL	100.4	100.7	99.9	100.0
100 Mg				
Mg+Fe	73.9	81.1	73.7	65.0
<i>Numbers of ions on the basis of 6 oxygens</i>				
Si	1.8456	1.8662	1.9135	1.8975
Al	0.1544	0.1338	0.0865	0.1025
Al	0.2116	0.1193	0.1136	0.1256
Ti	0.0326	0.0212	0.0245	0.0335
Fe	0.3263	0.3299	0.4470	0.4481
Mg	0.9265	1.4178	1.2492	0.8322
Ca	0.4140	0.0980	0.1276	0.4904
Na	0.0560			0.0253
Mg	55.6	76.8	68.5	47.0
Fe	19.6	17.9	24.5	25.3
Ca	24.8	5.3	7.0	27.7

\*Denotes calculated composition.

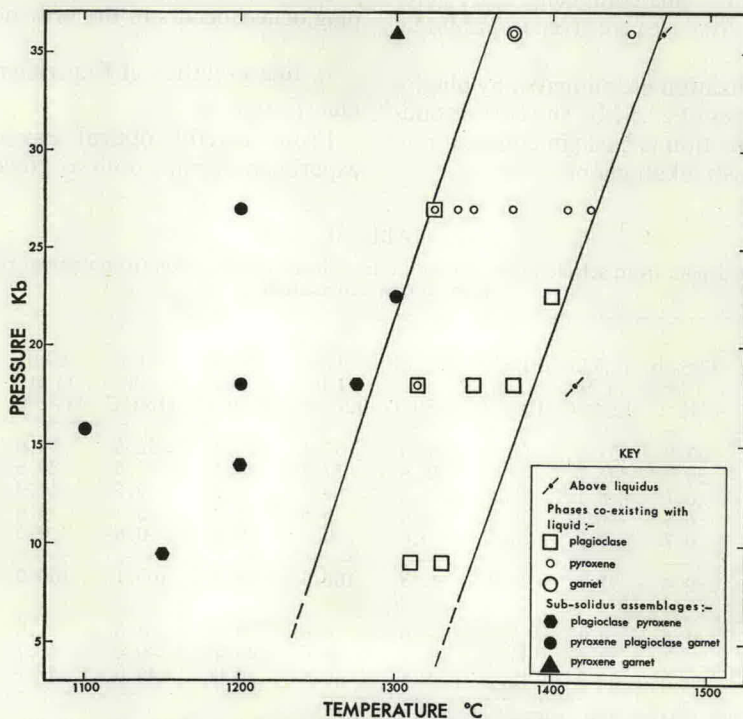


FIG. 2. Results of the experimental runs on the gabbroic anorthosite composition.